World Journal of Innovation and Modern Technology, Vol. 6, Issue 5, (Oct) 2023
ISSN 2682-5910
DOI: 10.53469/wjimt.2023.06(05).08

Multi-Beam Surveying Ocean Exploration Model and Applications

Dehao Wang, Hongyang Gao, Hang Zhang

School of Civil Engineering, University of Science and Technology Liaoning, Anshan, Liaoning, China
171562358@qq.com

Abstract: ***This article first explores the principles of bathymetric measurement using a multi-beam echo sounder system to analyze seafloor topography. It determines the water depth, coverage width of the multi-beam bathymetry, and the overlap rate between adjacent swaths. Subsequently, the article establishes mathematical calculation models for seafloor topography data under different conditions. Finally, by applying these models to computer-based analysis, accurate and practical conclusions and solutions are obtained, which are of reference value for the design of survey lines in multi-beam echo sounder systems.***

Keywords: seawater depth calculation model; coverage width calculation model; adjacent swath overlap rate calculation model; multi-beam survey line" or "multi-beam sounding line.

1. INTRODUCTION

With the development of ocean depth measurement technology, the application of multi-beam echo sounder systems in measuring water depth has become increasingly widespread. Single-beam sounding can calculate depth by emitting sound waves vertically towards the seafloor using a transducer on the survey vessel, based on the speed and time it takes for the sound waves to propagate through the water. The data distribution characteristic is that data is denser along the vessel's track, but there is no data between survey lines. Therefore, in areas with a flat seafloor, a multi-beam echo sounder system is used to measure full-coverage depth swaths with the survey vessel as the axis, and a certain width. This further calculates the overlap rate between survey lines when they are parallel and the seafloor is flat. To ensure a full-coverage measurement, there should be a 10% to 20% overlap rate between adjacent swaths. However, the actual seafloor terrain varies significantly, and whether using an average survey line spacing or the shallowest point survey line spacing, neither can guarantee the best measurement results.

Grządziel A [1] estimating the precise time required for multi-beam echo sounding measurements allows for effective planning of hydrographic survey projects, helping to avoid unnecessary costs and delays while improving efficiency. Guo Q[2] and others believe that dual-head multi-beam systems are better at representing seafloor topography and improving efficiency compared to single-head systems. Lu Z[3] and others believed that tidal actions significantly increase the release of polycyclic aromatic hydrocarbons (PAHs) from sediment into seawater, especially dissolved PAHs. Additionally, the concentration of PAHs is positively correlated with the suspended particulate matter content. Jia-Meng J[4] and others have conducted research to establish a water-bottom horizontal layer model suitable for deep-water environments. This model reveals that Scholte waves exhibit weaker dispersion characteristics in deep water and are influenced by factors such as water depth, seafloor physical parameters, and sound velocity. Specht M[5] and others researchers have found that measuring water depth with higher accuracy is possible in shallow waters, but the precision decreases in deep waters. Aranchuk V[6] and others have developed a new type of laser multi-beam differential interference sensor called LAMBDIS. It is insensitive to the sensor's own movement and can real-time detect buried objects. Chen X[7] and others believe that two independently reconfigurable beams can be generated at a fixed frequency. Aranchuk V[8] and others believe that the limitation of maximum measurable velocity can be overcome by selecting the beam spacing on the object and the displacement between camera images.. Xian P[9] and others proposed that using a constant seawater density would lead to errors in gravity gradients, and therefore, it is necessary to take into account the variations in seawater density. Wang J[10] and others proposed a multi-beam bathymetric method for AUVs (Autonomous Underwater Vehicles) operating in fixed-depth mode, with the aim of improving operational efficiency and data quality. Cui J[11] and others have provided an efficient and accurate method for shallow water depth inversion under complex hydrographic conditions. Qiang G[12] and others believe that A dual-head multi-beam echo sounder system, in comparison to a single-head system, is better at representing seafloor topography features, reducing survey time, decreasing labor intensity, and improving measurement efficiency. Tao S[13] and others analyzed the impact of temperature, salinity, and depth variations on the beam trigger point coordinates and quantified their effects. Temperature has the greatest impact on sound velocity, followed by salinity and depth. Wang S[14] and others

believe that multi-beam echo sounder systems have higher structural requirements for the objects being measured and provide moderate accuracy, making them more suitable for large-scale underwater obstacle measurements. Chen C[15] and others have found that combining a multi-beam echo sounder system with side-scan sonar can effectively leverage their complementary advantages and result in more detailed and accurate depth data.

Based on the current research status and the background of the problem, the main focus of this article is to establish a model for the coverage width and overlap rate between adjacent swaths in multi-beam bathymetry, as well as to develop a model for calculating the coverage width.

2. THE RESOLUTION OF THE COVERAGE WIDTH AND OVERLAP RATE BETWEEN ADJACENT SWATHS

2.1 Establishing a model for the estimation of seawater depth.

Seawater depth refers to the vertical distance between a vessel and the seafloor slope. In this article, a depth estimation model for seawater will be constructed based on the distance from the survey line to the center point and the slope, and the following definitions will be provided:

definition 1: x represents the distance between the survey line and the center point. It is stipulated that the sign carried by x before it represents the direction. x is positive when the survey line is on the left side of the center point. x = -800m, −600m, ..., 800m.

definition 2: l_x represents the survey line located at a distance of x meters from the center point, l_0 represents the survey line at the center point of the marine area.

Based on the defined variables above, a schematic diagram of the seawater depth estimation model is depicted in Figure 1.

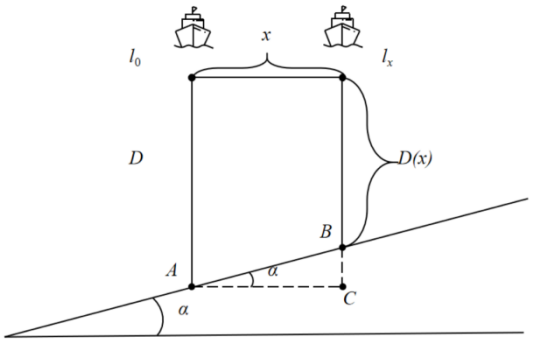

Figure 1: Schematic diagram of seawater depth estimation

As shown in Figure 1, α represents the seafloor slope. Points A and B represent the intersection of the vessel, located at the center of the marine area, and the point located x meters away from the center point, respectively. Point C represents the intersection of the extension of line A, parallel to the sea surface, with the extension of line B, perpendicular to the sea surface.

The calculation formula for seawater depth, $D(x)$, at a distance of x meters from the center point can be derived using the tangent function of the triangle, as shown in Equation (1).

$$D(x) = D - x\tan\alpha \tag{1}$$

Where D represents the seawater depth at the center point of the marine area, with a value of D = 70 m, and $D(x)$ represents the seawater depth at a distance of x meters from the center point, with the right side as the positive direction. x = −800m, −600m, ..., 800m.

2.2 Establishing a coverage width estimation model.

In this article, the coverage width estimation model is first established based on slope, opening angle, and the seawater depth at the center of the marine area. A schematic diagram of the coverage width estimation model is shown in Figure 2.

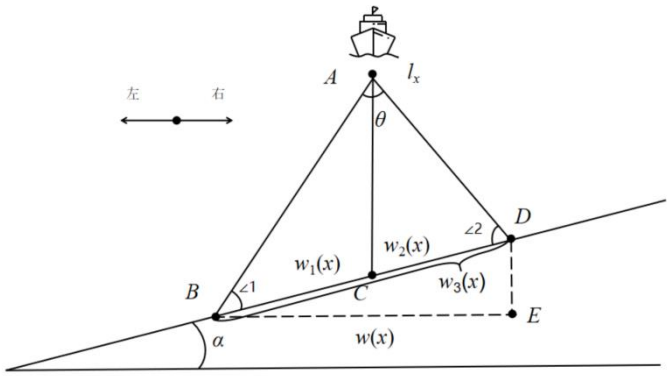

Figure 2: Schematic diagram of coverage width estimation model

As shown in Figure 2, θ represents the opening angle of the multi-beam transducer. Point A is the position of the vessel, while points B and D represent the intersections of the left and right boundaries of the conical beam with the seafloor slope, respectively. First, a line is drawn from point A, intersecting the seafloor slope at point C, perpendicular to the sea surface. This is then divided into the left slope coverage width BC and the right slope coverage width CD. A horizontal line is drawn through point A, intersecting the vertical line through point D at point E on the sea surface.

STEP1: Calculate $\angle ABD$, $\angle ADB$

$$\angle ABD = 90^\circ - \alpha - \frac{\theta}{2} \tag{2}$$

$$\angle ADB = 90^\circ + \alpha - \frac{\theta}{2} \tag{3}$$

STEP2: Calculate the total width covering the seafloor slope.

$$w_1(x) = D(x)\left(\frac{\sin\frac{\theta}{2}}{\sin(90^\circ - \frac{\theta}{2} - \alpha)} + \frac{\sin\frac{\theta}{2}}{\sin(90^\circ - \frac{\theta}{2} + \alpha)}\right) \tag{4}$$

Where, $w_1(x)$ represents the width covered on the seafloor slope by the beam emitted from survey line l_x. $x = -800m, -600m, ..., 800m$.

STEP3: Calculate the total width covering the seafloor plane.

$$w(x) = w_1(x)\cos\alpha \tag{5}$$

Where, $w(x)$ is the width of the slope coverage $w_1(x)$ projected onto the seafloor plane. $x = -800m, -600m, ..., 800m$.

2.3 Establishing a model for survey line overlap rate calculation.

The article presents a schematic diagram of the overlap rate calculation model between the current survey line and the previous one, as shown in Figure 3.

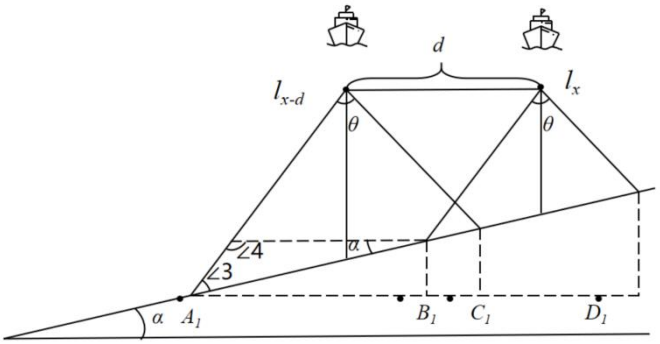

Figure 3: Schematic diagram of the overlap rate estimation model between adjacent swaths

From Figure 3, it can be observed that point A_1 is the intersection of the left boundary line of the beam emitted by survey line l_{x-d} and the seafloor slope. A parallel line to the sea surface is drawn through point A_1. A perpendicular line to the sea surface is drawn through the intersection of the right boundary line of the beam emitted by survey line l_{x-d} and the slope, and it intersects with the parallel line through A_1 at point C_1. Similarly, you can determine points B_1 and D_1 using the same principles.

STEP1: Calculate $\angle 3, \angle 4$.

$$\angle 3 = 90^\circ - \alpha - \frac{\theta}{2} \tag{6}$$

$$\angle 4 = 90^\circ + \frac{\theta}{2} \tag{7}$$

Where, $\angle 3$ represents the angle between the left boundary of the conical beam emitted by survey line l_{x-d} and the slope. $\angle 4$ represents the angle between the straight line between the two vessels and the left boundary of the conical beam. α represents the seafloor slope, and θ represents the opening angle of the multi-beam transducer.

STEP2: Calculate the non-overlapping coverage width A_1B_1.

$$A_1B_1 = d\frac{\sin(90^\circ + \frac{\theta}{2})}{\sin(90^\circ - \alpha - \frac{\theta}{2})}\cos\alpha \tag{8}$$

Where A_1B_1 represents the non-overlapping portion of the coverage width covered by survey line l_{x-d} on the seafloor plane compared to the coverage width of l_x and d denotes the distance between the current survey line and the previous one. $d = 200m$.

STEP3: Calculate the coverage width B_1C_1 that overlaps with the previous survey line.

$$B_1C_1 = w(x-d) - d\frac{\sin(90^\circ + \frac{\theta}{2})}{\sin(90^\circ - \alpha - \frac{\theta}{2})}\cos\alpha \tag{9}$$

Where $w(x)$ is the sum of the A_1B_1 segment and the C_1D_1 segment, and $w(x-d)$ represents the sum of the B_1C_1 segment and the A_1B_1 segment. $x = -800m, -600m, ..., 800m$.

STEP4: Calculate the overlap rate with the previous survey line.

In reality, most seafloor terrains are not flat but have a certain slope. Therefore, it is necessary to modify the formula accordingly.

$$\eta(x) = \frac{B_1C_1}{w(x)} \tag{10}$$

Where $\eta(x)$ represents the overlap rate between the survey line at a distance of x meters from the center point and the preceding survey line. $x = -800m, -600m, ..., 800m$, $d = 200m$.

3. THE RESOLUTION OF THE COVERAGE WIDTH PROBLEM WITH CHANGING SURVEY LINE DIRECTION

3.1 Establishing a rectangular marine area depth estimation model

This article aims to calculate the width of the beam coverage on the sea surface in the direction of the survey lines at various distances from the center of a rectangular marine area. Subsequent calculations will involve unit conversion (1 nautical mile = 1852 meters) and computing the seawater depth at various positions on the sea surface along the survey lines. Auxiliary lines will be drawn to indicate contour segments of seawater depth, as shown in Figure 4.

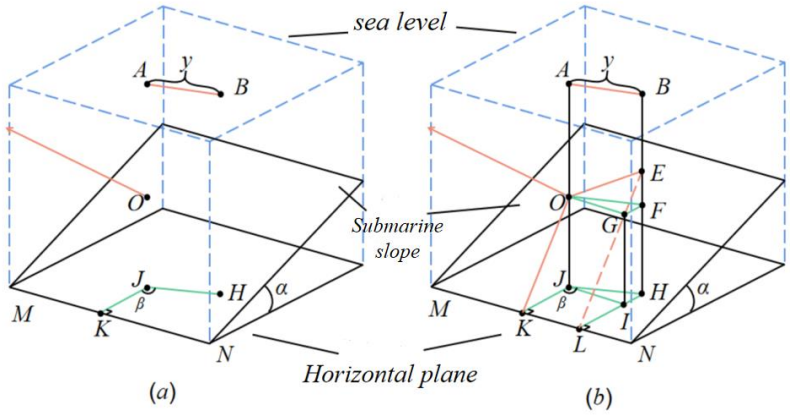

Figure 4: Schematic diagram of rectangular marine area depth

(1) The meaning of the various points in the diagram.

In Figure (*a*), point *A* represents the center of the marine area, point *B* is the position of the survey vessel, point *H* is the projection of point *B* onto the seafloor plane, point *J* is the projection of point *A* onto the seafloor plane, point *K* is the perpendicular point from point *J* to the boundary of the seafloor slope, line segment *JK* represents the projection of the seafloor slope's normal vector onto the horizontal plane, α is the slope of the seafloor slope, and β is the angle between the direction of the survey line and the projection of the seafloor slope's normal vector on the horizontal plane.

(2) Procedure for drawing auxiliary lines.

Connect point *A* to point *J*, intersecting the seafloor slope at point *O*. Connect point *B* to point *H*, intersecting the seafloor slope at point *E*. Draw a line parallel to segment *AB* through point *O*, intersecting *BH* at point *F*. Draw a perpendicular line to line *MN* through point *H*, intersecting *MN* at point *L*. Connect points *E* and *L*. Connect points *O* and *K*. Draw a line parallel to the sea surface through point *F*, intersecting *EL* at point *G*. Draw a perpendicular line to the sea surface through point *G*, intersecting *HL* at point *I*. Connect points *J* and *I*. This results in the rectangular shape in Figure (*b*).

(3) Model derivation.

Derive a model for seawater depth based on the above auxiliary lines.

STEP1: Proof $\triangle OGF \cong \triangle JIH$.

$$\begin{cases} FG \parallel HL \\ OF \parallel HJ \\ OF = HJ \\ FG = HI \end{cases} \tag{11}$$

STEP2: Proof $\angle KJI = 90°$.

$$\begin{cases} GI \perp \text{sea level} \\ OJ \perp \text{sea level} \\ OK \parallel EL \\ \Delta OGF \cong \Delta JIH \\ JI \parallel KL \\ JK \perp MN \end{cases} \tag{12}$$

According to equation (12), the transitivity of parallel lines and the supplementary angles formed by the corresponding interior angles of parallel lines can prove that $\angle KJI = 90°$.

STEP3: Calculate the value of FG.

$$\begin{cases} \angle HJK = \angle KJI + \angle HJI \\ \angle HJK = \beta \\ \Delta OGF \cong \Delta JIH \\ KJ \parallel HL \\ OF = y \end{cases} \tag{13}$$

According to equation (13) can calculate $FG = y\sin(\beta - 90°)$.

STEP4: Calculate EF.

$$\begin{cases} EH \perp \text{sea level} \\ HL \perp MN \\ FG \parallel HL \\ FG \in \Delta EHL \\ HL \in \Delta EHL \end{cases} \tag{14}$$

According to equation (14) can obtain $EF = y\sin(\beta - 90°)\tan\alpha$.

STEP5: Calculate the value of the seawater depth.

The formula for calculating the vertical distance to the seabed and, consequently, the seawater depth, is given by Equation (15).

$$D(y) = D - y\sin(\beta - 90^{\circ})\tan\alpha \tag{15}$$

Where D represents the water depth in the central area. $D = 120m$.

When the azimuth angle is 90° and 270°, the direction of the measurement line is parallel to the sea surface, and its slope angle is equal to the slope angle α mentioned in this paper. Therefore, the distance data between the measurement ship and the central point of the sea area and the calculated seawater depth are successively substituted into Equation (1) and Equation (5) to obtain the coverage width.

3.2 Establish a model for calculating the seabed slope angle.

To calculate the angle formed by the beam coverage on the seabed slope relative to the horizontal plane, draw auxiliary lines on the rectangular schematic diagram of the surveyed sea area provided in the question to indicate the slope angle and other parameters, as shown in Figure 5.

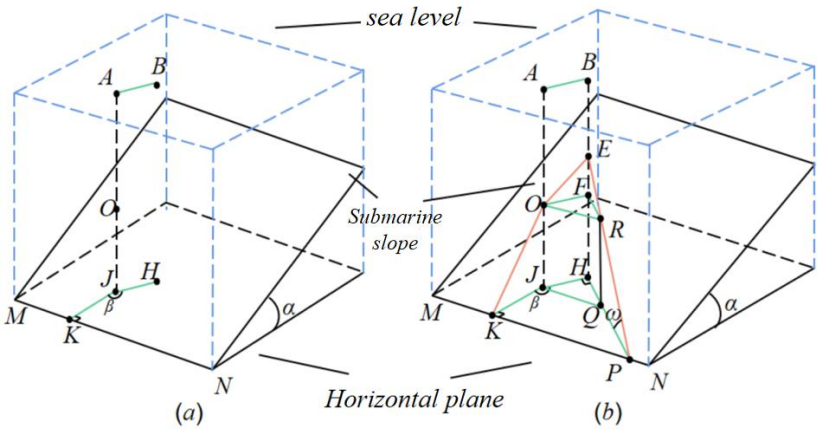

Figure 5: Rectangular Sea Area Slope Diagram

(1) The meaning of the various points in the diagram.

In the rectangle shown in Figure (*a*), the meanings of the points, line segments, α angle, and β angle are the same as in Figure 4.

(2) Procedure for drawing auxiliary lines.

Connect line segment *BH*, intersecting the slope surface at point *E*. Draw a parallel line to *AB* through point *O*, intersecting line *BH* at point *F*. Draw a perpendicular line to *HJ* through point *H*, intersecting line *MN* at point *P*. Draw a parallel line to *MN* through point *J*, intersecting line *HP* at point *Q*. Draw a parallel line to *JQ* through point *O*, intersecting line *EP* at point *R*. Connect *PR* and extend it to intersect *BH* at point *E*. Connect *OK* and *EO*. This results in the rectangle shown in Figure (*b*).

STEP1: Proof $\triangle OFR \cong \triangle JHQ$.

$$\begin{cases} OR \parallel JQ \\ OR = JQ \\ OF \parallel HJ \\ OF = HJ \end{cases} \tag{16}$$

STEP2: Calculate the value of $\angle FOR$.

$$\begin{cases} JQ \parallel MN \\ JK \perp MN \\ \angle KJH = \beta \\ \angle KJH = \angle KJQ + \angle HJQ \\ \Delta OFR \cong \Delta JHQ \end{cases} \tag{17}$$

According to equation (17) can obtain $\angle FOR = \beta - 90°$.

STEP3: Calculate the slope value ω.

$$\begin{cases} \angle FOR = \beta - 90^{\circ} \\ \Delta OFR \cong \Delta JHQ \\ HJ \perp HQ \\ OF = y \end{cases} \tag{18}$$

According to the Pythagorean theorem for a right triangle can obtain $FR = y \tan(\beta - 90°)$. Let $\angle ERF = \omega$, and calculate the slope using the azimuth angle and spatial geometric relationships. The formula for calculating the slope angle ω is as shown in Equation (19).

$$\omega = \arctan(\cos(\beta - 90^{\circ}) \tan \alpha) \tag{19}$$

Where ω represents the magnitude of the slope angle.

3.3 Establish a coverage width calculation model.

Given a multi-beam transducer with a beamwidth of 120°, a slope of 1.5°, and a seawater depth of 120m at the central point of the sea area, you can substitute the seawater depth $D(x)$ and the slope angle ω into the coverage width calculation model established in this paper. By using Equation (5), you can calculate the coverage width as it varies with the distance from the measurement ship to the central point of the sea area and the change in azimuth angle.

When the azimuth angle is 90° and 270°, the measurement line direction is parallel to the sea surface represented by MN. In this situation, the calculation of seawater depth follows the same method as the seawater depth measurement model presented in this paper. Therefore, by substituting the given conditions into Equation (1) and Equation (5), you can calculate the seawater depth and coverage width when the azimuth angle is 90° and 270°.

4. RESULTS AND ANALYSIS

4.1 Coverage width and overlap rate issues' results

Based on the provided data, it is known that the multi-beam transducer has a beam angle of θ=120°, a slope of α=1.5°, and the seawater depth at the central point of the sea area is D=70m. By inputting this data into the calculation model, you can compute the seawater depth at different distances from the center point, the coverage width, and the overlap rate. The calculation results are shown in Table 1.

Table 1: The indicator values at the listed positions

The distance from the measuring line to the center point / m	-800	-600	-400	-200	0	200	400	600	800
Ocean water depth / m	90.95	85.71	80.47	75.24	70.00	64.76	59.53	54.29	49.05
Coverage width / m	315.71	297.53	279.35	261.17	242.99	224.81	206.63	188.45	170.27
The overlap rate with the previous survey line / %		36.70	31.51	26.74	21.26	14.89	7.41	-1.53	-12.36

According to Table 1, it is evident that, with survey line l_0 as the center, the ocean water depth measured by survey lines to the left is deeper, while the ocean water depth measured by survey lines to the right is shallower. This indicates that the seafloor surveyed in this depth measurement consists of a slope that descends from left to right. The coverage width of the swath is widest at the leftmost survey line, measuring 315.71m, and it becomes narrower as you move to the right, with the narrowest coverage width of 170.27m at the rightmost survey line. This is because the multibeam depth measurement system emits conical beams with a smaller beam angle in the upper direction and a larger one in the lower direction. As the seafloor slope rises progressively from left to right, it results in decreasing swath width on the slope.The actual seafloor terrain is diverse and complex. To ensure measurement accuracy, there should be a 10% to 20% overlap between adjacent swaths. In the case of survey lines at 600m and 800m from the center, a negative overlap rate was observed with the preceding survey line, indicating that there were gaps in the measurements at these locations, which are 400m and 600m from the center, respectively.

At distances of $-800m$, $-600m$, $-400m$ and $-200m$ from the center, the overlap rate with the preceding survey line exceeded 20%. This is because the water depth is deeper in these areas, leading to excessive overlap in swath coverage.

4.2 The results of the coverage width variation issue in the direction of survey lines

Using the distance between the measurement vessel and the center point of the sea area, as well as the angle between the survey line direction provided in the question, we calculated the coverage width using the coverage width model. The results of the multibeam depth measurements at the listed positions are shown in Table 2.

Table 2: Coverage width

Coverage width/m		The distance from the measurement vessel to the center point of the sea area/Nautical miles							
		0	0.3	0.6	0.9	1.2	1.5	1.8	2.1
The angle of the survey line direction /°	0	415.6922	466.0911	516.4899	566.8888	617.2876	667.6865	718.0854	768.4842
	45	416.1202	451.7943	487.4683	523.1424	558.8165	594.4905	630.1646	665.8387
	90	416.5491	416.5491	416.5491	416.5491	416.5491	416.5491	416.5491	416.5491
	135	416.1202	380.4461	344.7721	309.0980	273.4239	237.7498	202.0758	166.4017
	180	415.6922	365.2933	314.8945	264.4956	214.0967	163.6979	113.2990	62.9002
	225	416.1202	380.4461	344.7721	309.0980	273.4239	237.7498	202.0758	166.4017
	270	416.5491	416.5491	416.5491	416.5491	416.5491	416.5491	416.5491	416.5491
	315	416.1202	451.7943	487.4683	523.1424	558.8165	594.4905	630.1646	665.8387

From Table 2, it is evident that when the survey line direction angle is 90° and 270°, the survey line direction is parallel to the *MN* plane in the horizontal plane. Therefore, at any distance from the measurement vessel to the center of the sea area, the swath's coverage width, denoted as $w(x)$, remains constant. When the survey line direction angles are 0°, 45°, 135°, 180° and 225°, the coverage width of the swath decreases as the distance from the measurement vessel to the center of the sea area increases. Conversely, when the survey line direction angle is 315°, the coverage width of the swath increases as the distance from the measurement vessel to the center of the sea area increases.

REFERENCES

[1] Grządziel A. Method of Time Estimation for the Bathymetric Surveys Conducted with a Multi-Beam Echosounder System[J]. Applied Sciences, 2023, 13(18): 10139.
[2] Guo Q, Fu C, Chen Y, et al. Application of multi-beam bathymetry system in shallow water area[C]//Journal of Physics: Conference Series. IOP Publishing, 2023, 2428(1): 012042.
[3] Lu Z, Tian W, Zhang S, et al. A study combining a sediment-seawater microcosm with multimedia fugacity model to evaluate the effect of tidal cycles on polycyclic aromatic hydrocarbon release from sediments[J]. Science of The Total Environment, 2023, 891: 164340.
[4] Jia-Meng J, Peng-Fei Y. Dispersion characteristics of seabed Scholte waves with variable velocity seawater in deep water[J]. Applied Geophysics, 2023: 1-16.
[5] Specht M, Szostak B, Lewicka O, et al. Method for determining of shallow water depths based on data recorded by UAV/USV vehicles and processed using the SVR algorithm[J]. Measurement, 2023, 221: 113437.
[6] Aranchuk V, Johnson S, Aranchuk I, et al. Laser Doppler multi-beam differential vibration sensor based on a line-scan CMOS camera for real-time buried objects detection[J]. Optics Express, 2023, 31(1): 235-247.
[7] Chen X, Liu J. Tunable Multi-Beam Periodic Leaky-Wave Antenna Based on Radiation of Multiple Space Harmonics[J]. IEEE Antennas and Wireless Propagation Letters, 2023.

[8] Aranchuk V, Kasu R, Li J, et al. Application of line-scan CMOS camera in multi-beam heterodyne differential laser Doppler vibration sensor[J]. Optics Letters, 2023, 48(10): 2724-2727.
[9] Xian P, Ji B, Bian S, et al. Influence of Differences in the Density of Seawater on the Measurement of the Underwater Gravity Gradient[J]. Sensors, 2023, 23(2): 714.
[10] Wang J, Tang Y, Jin S, et al. A Method for Multi-Beam Bathymetric Surveys in Unfamiliar Waters Based on the AUV Constant-Depth Mode[J]. Journal of Marine Science and Engineering, 2023, 11(7): 1466.
[11] Cui J, Luo X, Wu Z, et al. High-Precision Inversion of Shallow Bathymetry under Complex Hydrographic Conditions Using VGG19—A Case Study of the Taiwan Banks[J]. Remote Sensing, 2023, 15(5): 1257.
[12] Qiang G,Chuanyu F,Yikang C, et al. Application of multi-beam bathymetry system in shallow water area[J]. Journal of Physics: Conference Series,2023,2428(1).
[13] Tao S, Linbang H. Analysis of the influence of temperature, salinity and depth variations on beam footprint coordinates[J]. Haiyang Xuebao, 2023, 45(2): 130-138.
[14] Wang S, Rong Y, Jiang H, et al. Comparison of multi-beam bathymetric system and 3D sonar system in underwater detection of beach obstacles[C]//Journal of Physics: Conference Series. IOP Publishing, 2021, 1961(1): 012034.
[15] Chen C, Tian Y. Comprehensive application of multi-beam sounding system and side-scan sonar in scouring detection of underwater structures in offshore wind farms[C]//IOP Conference Series: Earth and Environmental Science. IOP Publishing, 2021, 668(1): 012007.